

Energy spectra of trapped electrons and positrons with $E > 50$ MeV measured by the PAMELA magnetic spectrometer

V.V. Mikhailov¹, A. Bruno^{2,*}

for PAMELA collaboration

¹ National Research Nuclear University MEPhI (Moscow Engineering Physics Institute), Russia

² Heliophysics Division, NASA Goddard Space Flight Center

E-mail: vvmikhajlov@mephi.ru

Trapped electrons and positrons in the Earth inner radiation belt were observed by the PAMELA experiment on board Resurs DK satellite. The instrument consists of magnetic spectrometer, imaging electromagnetic calorimeter, time of flight system, anticoincidence and neutron detectors that provide unique particle identification and background rejection in wide energy range from 50 MeV up to hundreds GeVs. PAMELA was collecting data since June 2006 till January 2016. The satellite orbit with 350-600km initial altitude and 70° inclination crosses the inner radiation belt in South Atlantic Anomaly at L-shell 1.2. The trajectories of trapped electrons and positrons in the Earth magnetic field were reconstructed by means of a trajectory tracing simulation. In this work PAMELA's spectral measurements are compared with those of other spacecraft and with theoretical predictions.

*36th International Cosmic Ray Conference -ICRC2019-
July 24th - August 1st, 2019
Madison, WI, U.S.A.*

*Speaker.

1. Introduction

High energy galactic particles can penetrate magnetic field of the Earth and interact in atmosphere producing secondary particles including protons, electrons and positrons that, if originated with appropriate pitch angle, are trapped by the magnetic field forming long lived radiation belts in the Earth vicinity. Inner belt is mainly composed by high energy protons with energies up to a few GeVs [1] and electrons up to several MeVs. Flux of secondary high energy electrons above 100 MeV was first calculated in paper [2]. Namely in this work it was considered process of decay of charged pions produced in inelastic interactions of cosmic ray protons with residual atmosphere. Due to charge conservation there is small (about 1.2) excess of positive secondary particles. Pions decay through $\pi^\pm \rightarrow \mu^\pm \rightarrow e^\pm$ chain contributes to electrons and positrons. Intensity of this source is proportional to atmospheric density and lifetime is inversely proportional to density, so electrons and positrons form a halo around the Earth up to thousands kilometers.

Nuclear interactions of trapped protons of energies >300 MeV in upper atmosphere could also contribute to production of positrons and electrons in the innermost magnetosphere. Calculations performed in paper [3] predict the existence of a positron belt in a narrow region around L-shell = 1.2. The flux ratio of positrons to electrons e^+/e^- is estimated to be ~ 4 for energies of 40-1500 MeV. This mechanism exhibits sharply decreasing spectrum. At 200-300 MeV energies, positron fluxes from the trapped proton source are still comparable with the cosmic ray born positrons, but at greater energies production by trapped protons is negligible.

The magnetic spectrometer PAMELA was launched onboard the Resurs-DK1 satellite on the 15th of June 2006 and it was continuously taking data during 3200 days till January 2016. The satellite had a quasi-polar (70° inclination) elliptical orbit at an altitudes between 350 and 600 km. In September 2010 orbit was changed to circular with altitude 576 km. Preliminary results of the PAMELA observations of trapped electron and positron fluxes near the Earth, which were made in first years of the flight, were reported in papers [5]. These results show features of spectra for different geomagnetic regions due to their origin. Primary particles were observed mainly in polar region and above cut-off rigidity near equator. Secondary component prevails near equator below geomagnetic cut-off at low rigidities and trapped particles can be measured in South Atlantic Anomaly (SAA) with pitch-angles around 90° . Fluxes of trapped electrons and positrons in SAA are much higher than fluxes in equatorial region outside anomaly. Moreover, for trapped component an excess of electrons above model prediction was found at L-shell 1.2. This excess was increasing at top of drift shell at minimal values of local magnetic field B [6] in contradiction with calculations performed in paper [3].

This work presents PAMELA spectrometer measurements of spatial and energy distributions of trapped electrons and positrons for full set of data.

2. PAMELA spectrometer

The instrument consists of a Time-of-Flight system (TOF), an anticoincidence system (AC), a magnetic spectrometer, an electromagnetic calorimeter, a shower tail catching scintillator S4 and a neutron detector (ND) [7]. The TOF system provides the main trigger for particle acquisition, measures the absolute value of the particle charge and its flight time while crossing the apparatus

(the accuracy is better than 350 psec). Particle rigidity is determined by the magnetic spectrometer, composed by a permanent magnet with a magnetic field intensity 0.4 T and a set of six micro-strip silicon planes. The spatial resolution of the tracker system of the spectrometer was observed to be about $\sim 4 \mu\text{m}$, corresponding to a maximum detectable rigidity exceeding $\sim 1 \text{ TV}$. The high energy electron and positron identification is provided by the electromagnetic imaging calorimeter. The calorimeter consists of 44 layers with silicon detectors interleaved by 22 tungsten planes. Total thickness of calorimeter is 16.3 radiation and 0.6 nuclear interaction lengths. Particles not cleanly entering the PAMELA acceptance are rejected by the anticoincidence system. Neutron detector and shower scintillator improve particle identification. Using of the TOF system, the magnetic spectrometer and the calorimeter information allows electrons and positrons identification and determination of their energy from several tens MeV up to hundreds GeV. The acceptance is about $21.6 \text{ cm}^2\text{sr}$ [7].

The main axis of the PAMELA instrument was pointed mainly to a local zenith during the flight. The satellite attitude information and tracker data of the magnetic spectrometer gives possibility to determine detected particle direction in Greenwich system with accuracy about 2 degree. Orbit characteristics allow measuring particles with pitch angles (the angle between the particle velocity and the magnetic field vector) of about $80 - 90^\circ$ in the equatorial region at $L\text{-shell} \sim 1.2$. The angle between the main axis of the PAMELA spectrometer and magnetic field decreases with latitude, so for middle and high latitudes it is possible observe only small pitch angles.

3. Data analysis

Using the PAMELA data of 10^h data reduction for each registered event were obtained the number of tracks and energy losses in the magnetic spectrometer planes, rigidity, the time of flight, energy deposit in calorimeter strips and some others parameters. Only events with one track that have at least 4 points in bending projection X of the tracker were used in this analysis. Electrons and positrons were identified using information about dE/dx energy losses in the spectrometer planes to determine charge $Z = 1$, shower properties in the electromagnetic calorimeter, particle velocity and a rigidity. The misidentification of protons and, at low energies, pions is the largest source of background. At low energies to reduce background from interacting particles only events with no AC, ND and S4 signals were used.

The selection efficiency of electrons and rejection power of protons were estimated with Monte-Carlo simulation with official PAMELA Collaboration software [7]. Rejection power is about 10^4 for protons with energy below several GeVs which gives an estimate of the residual background of no more than a few percent. An unfolding procedure was applied for spectrum reconstruction to take into account energy resolution of the magnetic spectrometer.

Using a geographical coordinates and an orientation of PAMELA as a function of time, the McIlvain geomagnetic coordinates $L\text{-shell}$ and B were calculated for every event. For the calculation, the IGRF model (<http://nssdcftp.gsfc.nasa.gov/models/geomagnetic/igrf>) of the Earth magnetic field was used. The backtracking procedure was applied for every identified events to obtain trajectory of events in the Earth magnetosphere before detection. The integration was performed with a fourth-order Runge-Kutta method. Particles were followed up to 70 second that corresponds to drift time around the Earth of 70 MeV electrons. The tracing was stopped if particles touched

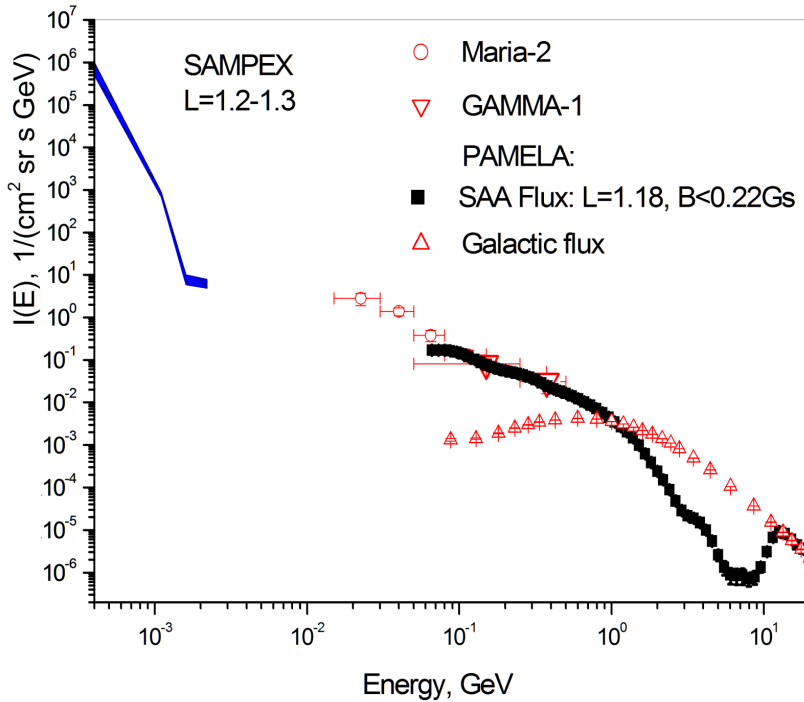


Figure 1: Differential energy spectrum of electrons and positrons (black squares) at L -shell 1.14-1.18, $B < 0.2$ Gs. For comparison data of GAMMA 1 and Maria-2 [9] and SAMPEX [10] in inner radiation belt and PAMELA data outside belt (filled circles for polar caps and gray points for equator) are shown

the Earth atmosphere at 40 km altitude or escaped magnetosphere. Escaping boundary was chosen to be 20000 km. Trajectory tracking allows to determine particle origin for every individual event. Primary electrons and positrons were excluded from analysis together with particles in transition region near geomagnetic cut-off, applying condition for particle rigidity $R < 10/L^3$ [GV]. Tracking of positrons and electrons with rigidity below cut-off clearly separates them in three different categories. First, particles with very short lifetime (less than 1 s) which were absorbed in opposite hemisphere after first bounce. For relativistic electrons and positrons this flight time does not depend from particle's rigidity. Second, particles with lifetime about 1 s, points of origin for this sample lie far from the satellite position on the other longitudes. If secondary electron or positron has appropriate pitch-angle to be mirrored by magnetic field, flight time increases due to drift around the Earth. Drift speed is increasing with increasing of particle rigidity. Typically, secondary particle absorbed after several bounces in mirror points, so the flight time of such quasitrapped particles is finite and it decreasing with rigidity. Such behavior of secondary albedo and quasitrapped electrons and positrons corresponds to that was observed in AMS-01 experiment [8] where they were called as short-lived and long-lived second leptons; Third, trapped particles with long flight time. In this case impossible to determine the full drift time and point of particle origin by simple tracing procedure because particles may make many revolution around the Earth and may stay trapped for minutes, hours, days and, perhaps, years. The known flight time gives possibility to separate particles of different origin detected in the same geographical region. In this

analysis electrons and positrons were classified as "trapped" if they performed at least one full drift around the Earth and their flight time exceeds 70 second.

4. Results

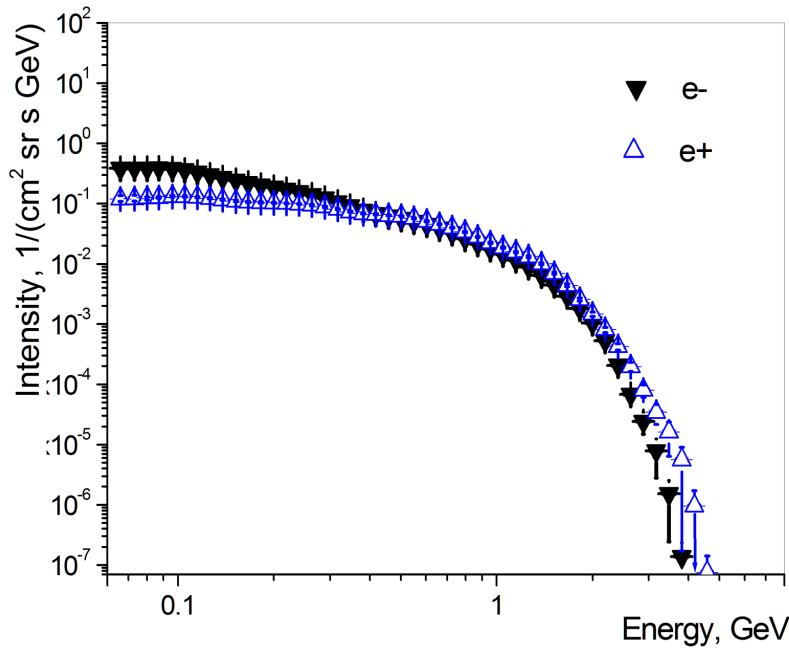


Figure 2: Differential energy spectra trapped positrons (open points) and electrons (filled points) at L -shell 1.14-1.20, $B < 0.21$ Gs .

In figure 1 differential energy spectrum of total electron and positron flux measured by the PAMELA magnetic spectrometer at region with geomagnetic coordinates $L = 1.15$ - 1.25 , $B < 0.21$ Gs is presented. This region corresponds SAA, where the PAMELA may detect trapped component with pitch-angles about 90 degrees. For comparison the figure shows also spectrum of galactic cosmic rays measured in polar region and data of other experiments in SAA [9, 10]. At low energies fluxes measured by SAMPEX vary significantly with time during solar cycle. Figure 1 shows interval between minimum in 2006 and maximum in 1997. Data corresponds to L -shell 1.3 [10]. Maria-2 and GAMMA-1 spectra were obtained at L -shell 1.2 in SAA [9]. The spectral shape above ~ 100 MeV is in agreement with calculation based on cosmic ray interaction with residual atmosphere. But at low energies electron to positron ratio increases. In paper [6] it was found that maximum of electron count was observed at L -shell about 1.17 at minimal value of magnetic field B available for measurements by PAMELA orbit. Figure 2 shows energy spectra of trapped electrons and positrons in region $L = 1.16$ - 1.18 , $B < 0.21$ Gs. Trapped particles are selected based on backtracing procedure as described above. Exposure time and efficiencies for electrons and positrons were taken the same as for all components spectrum measured in the same region. Only

statistical errors are shown. From figure 2 one can conclude that trapping component exists up to 2-3 GeV. Trapped spectra have sharp edge at about 2 GeV both for electrons and positrons. Clear excess of electrons is visible below energy $E \sim 300$ MeV which can not be explained with the cosmic ray production mechanism [12]. It is known that at low energies cosmic ray albedo neutron decay (CRAND) mechanism is main source of trapped protons but for electrons this source is not significant. Meanwhile, some estimations predict that CRAND may be the dominant source of inner radiation belt electrons in MeV energy range [11]. CRAND model predicts power law spectrum with index ~ 4 [11] that is too soft to explain experimental data above 10 MeV. An additional source of electrons could be due to high energy positron scattering on electrons of residual atmosphere [12].

5. Summary

New particle selection was applied to PAMELA data to obtain clean sample of electrons and positrons above 50 MeV. Using backtracking procedure over $\sim 2 \cdot 10^6$ electrons and positrons trapped component was separated and analyzed. Energy spectra of the trapped electrons and positrons have slope similar to quasitrapped component but with higher intensity and cut-off at about 2 GeV both for electrons and positrons. Below ~ 300 MeV excess of electrons over positrons which can not be explained by existing cosmic ray production mechanism models. More careful analysis of sources, trapping conditions and energy losses is necessary to understand origin of trapped high energy electrons and positrons in the inner radiation belt [12].

6. Acknowledgments

We acknowledge partial financial support from RFBR (grant 18-02-00656), the Ministry of Science and High education RF (project 3.2131.2017).

References

- [1] O. Adriani et al. [PAMELA collaboration]. *Astrophys. Journal Lett.* **v.799**, L4, 1 (2015).
- [2] N.L. Grigorov, Paper of AS USS. **24**, 810, (1977).
- [3] A.A. Gusev, U.B. Jayanthet, I.M. Martin, G.I. Pugacheva. *Journal of Geophys. Res.*, **v.106**, 11, A26111 (2001).
- [4] A.A. Gusev, U.B. Jayanthet, I.M. Martin, G.I. Pugacheva. *Geofisica Internacional* **v.109**, 11, A26111 (2004).
- [5] O. Adriani et al. [PAMELA collaboration]. *Phys. Rep.* **v.116**, 24, 241105 (2014).
- [6] V. Mikhailov et al.[PAMELA collaboration]. *PoS. 2017*, **v.100** (2017).
- [7] P. Picozza ,A.M. Galper, G. Castellini et al.[PAMELA collaboration],*Astropart. Phys.* **v.27**, 296 (2007).
- [8] Alcaraz, J., et al. [AMS-01 collaboration] *Phys. Lett. B*,**v. 484**, 10 (2000).
- [9] A. M. Galper, V. V. Dmitrenko, V. M. Gratchev et al. in *Radiation Belts: Models and Standards Geophysical Monograph 97*, p.129 (1997).

- [10] R. Selesnick, Journal of Geophys. Res. **v.120**, 8339 (2015).
- [11] R. Selesnick, Journal of Geophys. Res. **v.120**, 2912 (2015).
- [12] J.V. Mikhailova, A.M.Galper, V.V.Mikhailov. Phys. Atomic Nucl. **v.81**, 4 , 520 (2018).

POS (ICRC2019) 1122